

INTRODUCTION

The Multi-Object Broadband Imaging Echelle (MOBIE) is the seeing-limited, optical spectrograph planned for the first generation of Thirty Meter Telescope (TMT) instruments¹. The MOBIE instrument is currently in the conceptual design phase. This paper documents the progress to date on the stray light analysis of the imaging mode configuration. The goal of the stray light analysis at this phase of the project cycle is to provide a baseline estimate of the expected stray light background. To this end, four stray light calculations have been completed:

- Identification of critical objects;
- Estimated stray light background
- Off-axis rejection characteristics; and
- Ghost image formation.

The analyses are based on end-to-end ray traces of a complete, albeit reduced, system model that includes the Calotte-style dome, telescope optics and support structure, the MOBIE instrument optics and enclosure.

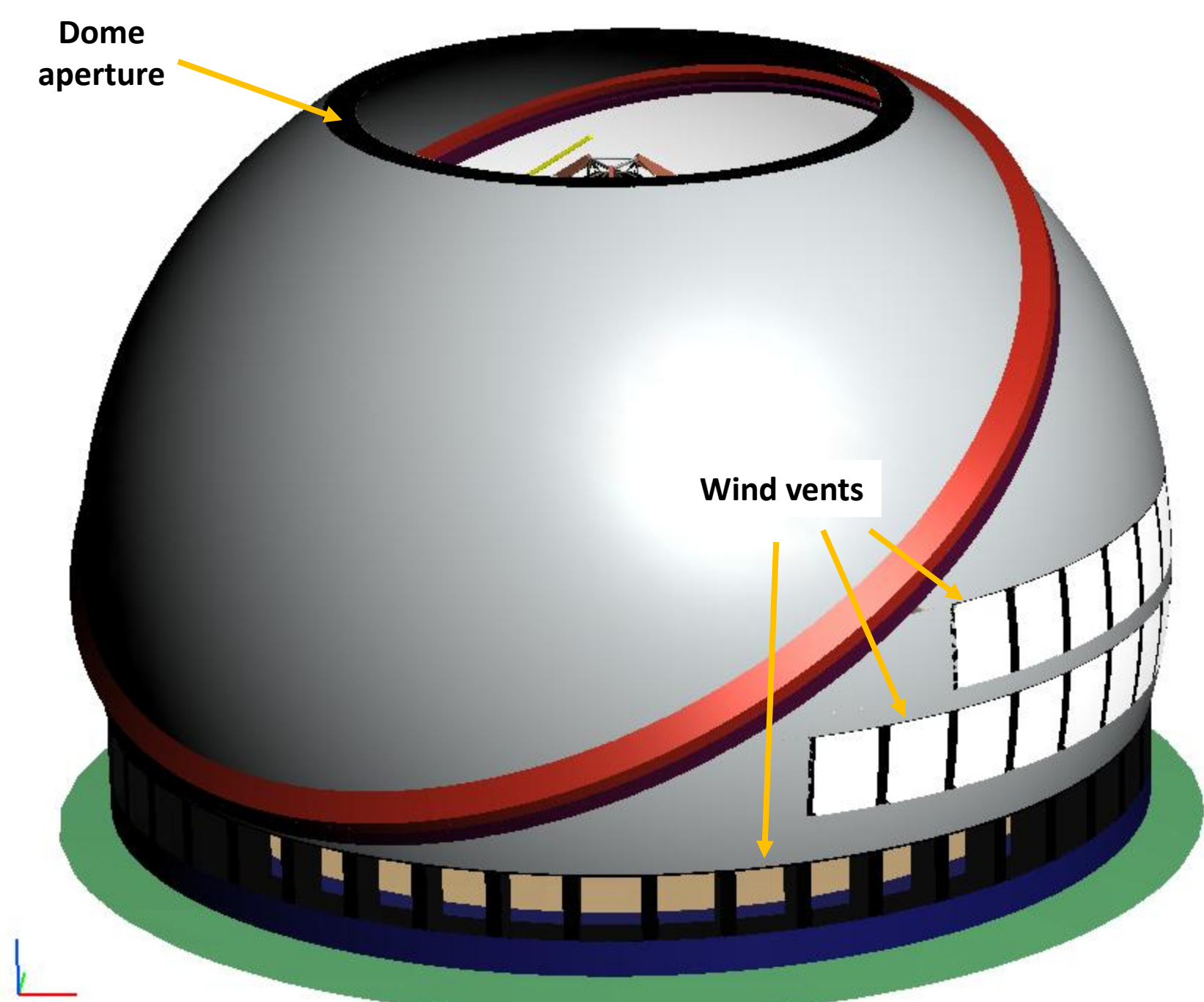


Figure 1. Complete TMT-MOBIE stray light analysis model

TMT-MOBIE GEOMETRY MODEL

The end-to-end system model is shown in Fig. 2 (the dome walls are hidden). The imaging mode configuration of the MOBIE instrument is shown in Fig. 3. A pair of atmospheric dispersion correction (ADC) prisms is located just prior to the field stop aperture. The field stop is a curved mask matching the curvature of the TMT focus surface and transmitting a 5.4 ± 2.1 arc minute by ± 4.8 arc minute rectangular field of view. The field stop is the principal stray light control mechanism inside the instrument. A reflective collimator (MC-1) follows the field stop. A dichroic beam splitter transmits and reflects light into the red and blue camera assemblies, respectively. It is subsequently folded into the refractive camera assemblies

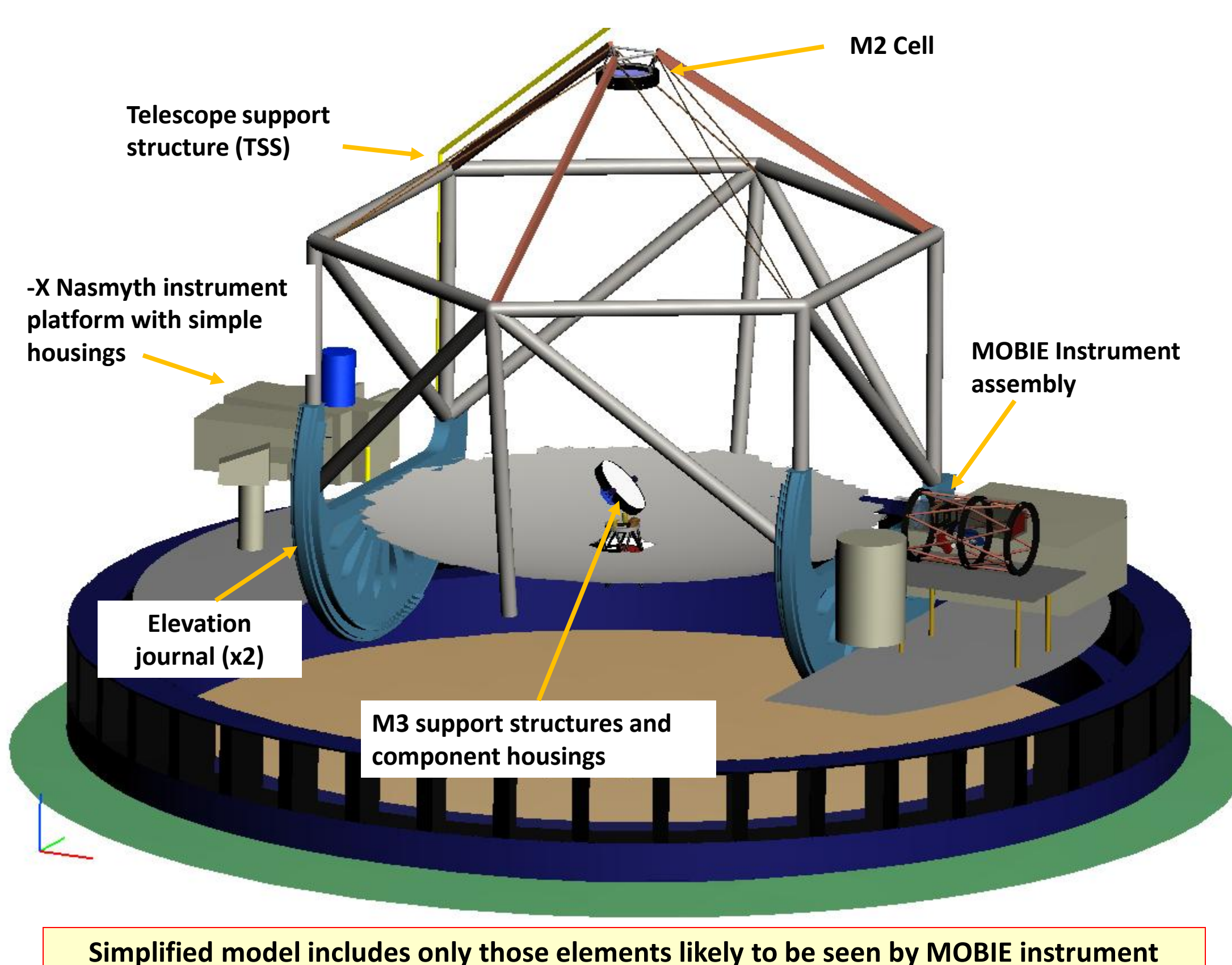


Figure 2. Dome interior

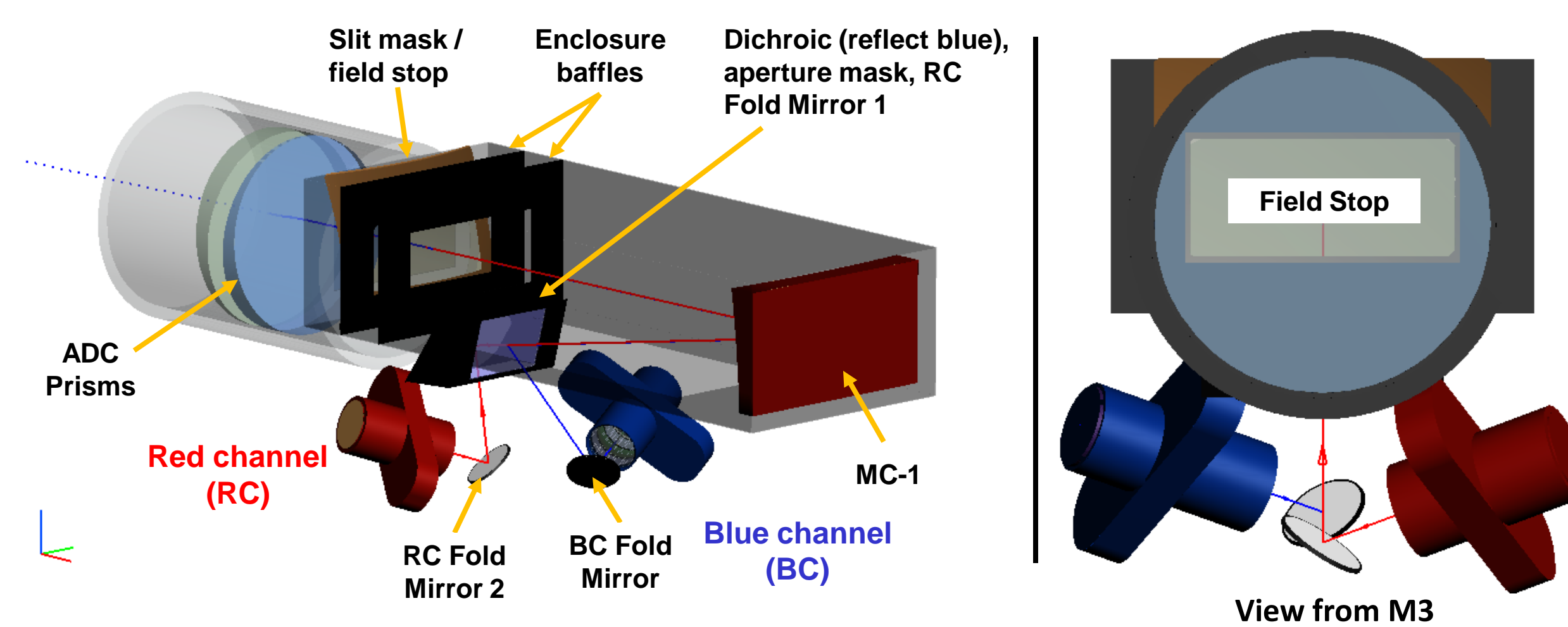


Figure 3. MOBIE instrument model

SURFACE PROPERTY ASSIGNMENTS

The mirror surfaces have a thin film aluminum coating, averaging 90% reflectivity across the instrument pass band. The lens surfaces have idealized anti-reflection coatings, reflecting 1% of the incident flux at each interface. The optical surfaces are assigned two scatter functions. A Harvey² BSDF simulates the scatter due to RMS micro-roughness³. A Mie scatter model using an IEST-STD-1246D particle size distribution function simulates the scatter due to particulate contamination^{4,5}. Non-optical surface treatments vary from flat black paint to glossy white.

ANALYSIS RESULTS

The critical/illuminated object analysis showed that light entering from outside the field of view has no direct path to the cameras. The cameras see the telescope support structures in the vicinity of M2 and M3, the elevation journals, and the dome floor. All of these objects are illuminated by external sources, with light entering through the top of the dome or in through the wind vents arranged around the dome walls.

With a black dome interior, stray light accounts for 4.0% of the total flux reaching the blue camera detector plane. The blue camera sees a strong red ghost reflection from the dichroic beam splitter. Absent this contribution, the background is reduced to 3.2%. The scattered light background is 2.8%. Under the same conditions for the red camera, stray light accounts for 3.7% of the total flux reaching the detector plane. The scattered light background is 3.3% of the total. Most of the contribution originates from sources within the sensor field of view. A white dome interior adds 0.3% to the scattered light background in both camera paths.

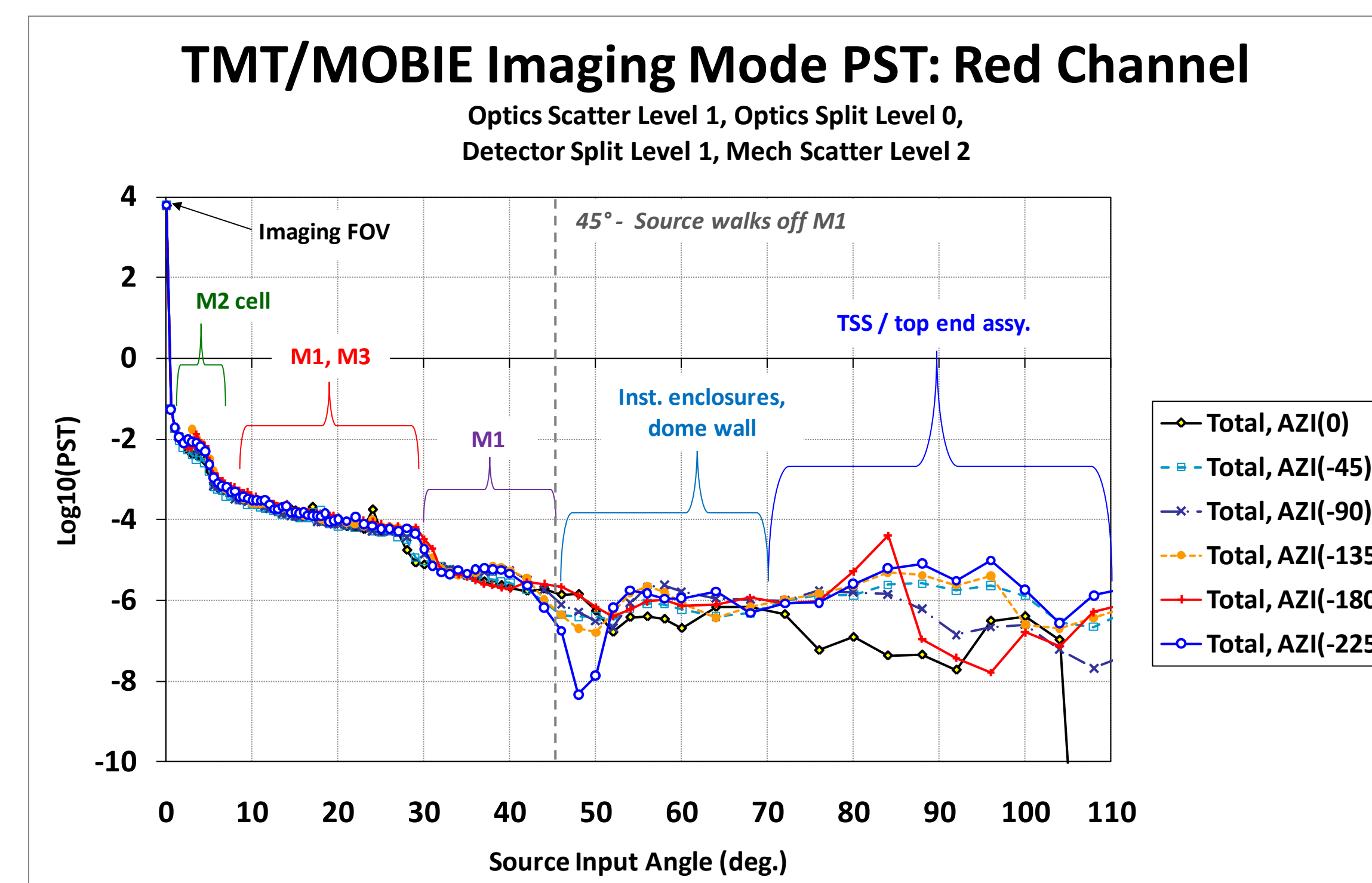
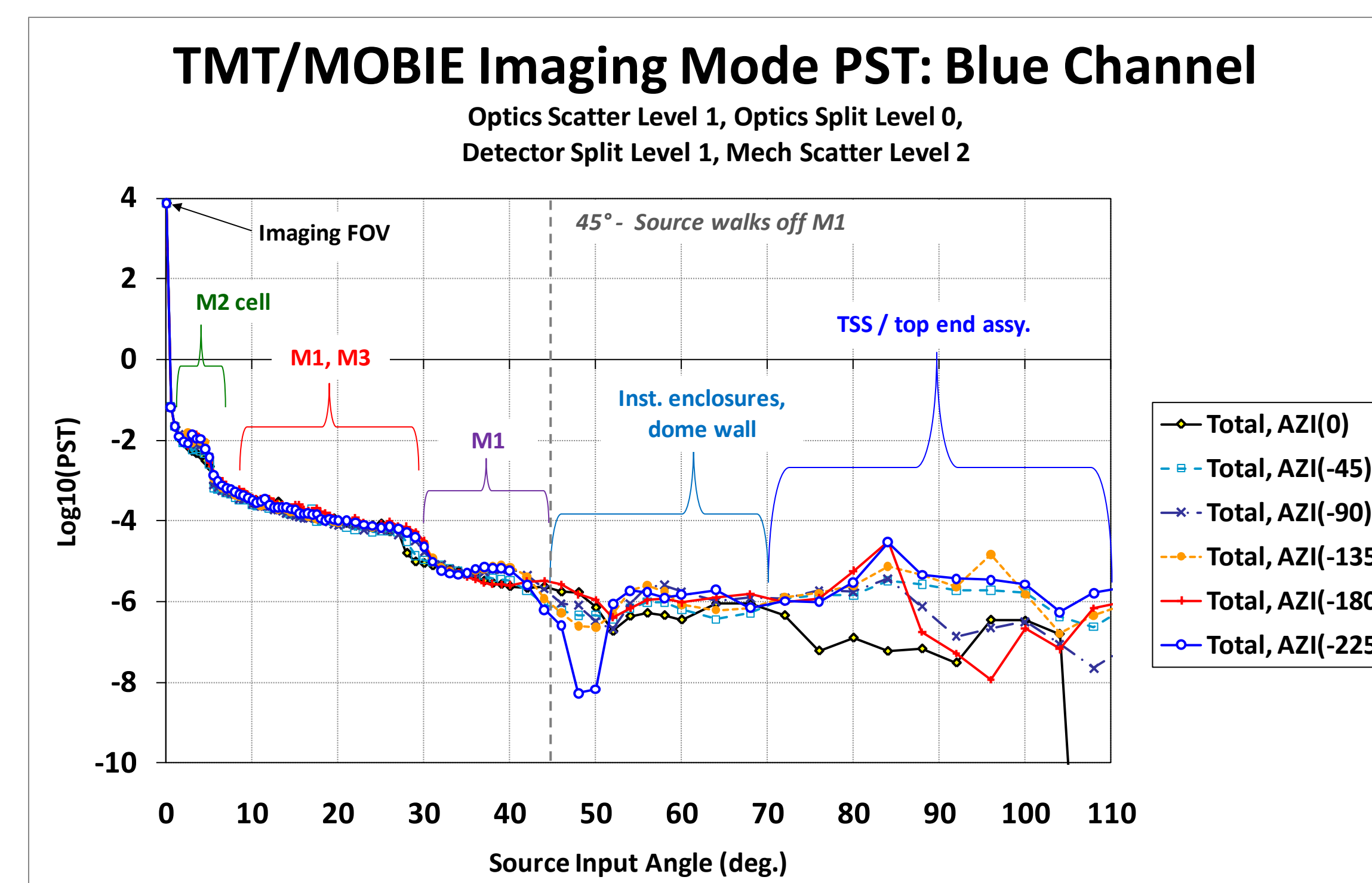


Figure 4. PST analysis results (blue – top; red – bottom)

Fig. 4 show the log space plots of the PST curves for the blue and red cameras, respectively. The PST analysis provides a way to quantify the out of field rejection characteristics of the telescope and instrument. The annotations on the plot indicate the most significant contributors to the stray light background over the range of angles indicated. The most important features to note are that there are no direct specular paths into the cameras from outside the instrument field of view and that scatter from the telescope optics and dome account for nearly all of the stray light background for objects outside the instrument field of view.

Fig. 5 shows log space ghost image irradiance plots at the camera sensor planes from source directions located inside the field of view. The ADC prisms produce image artifacts above and below the main image. The blue camera sees a strong red reflection from the dichroic beam splitter that overlays the direct image.

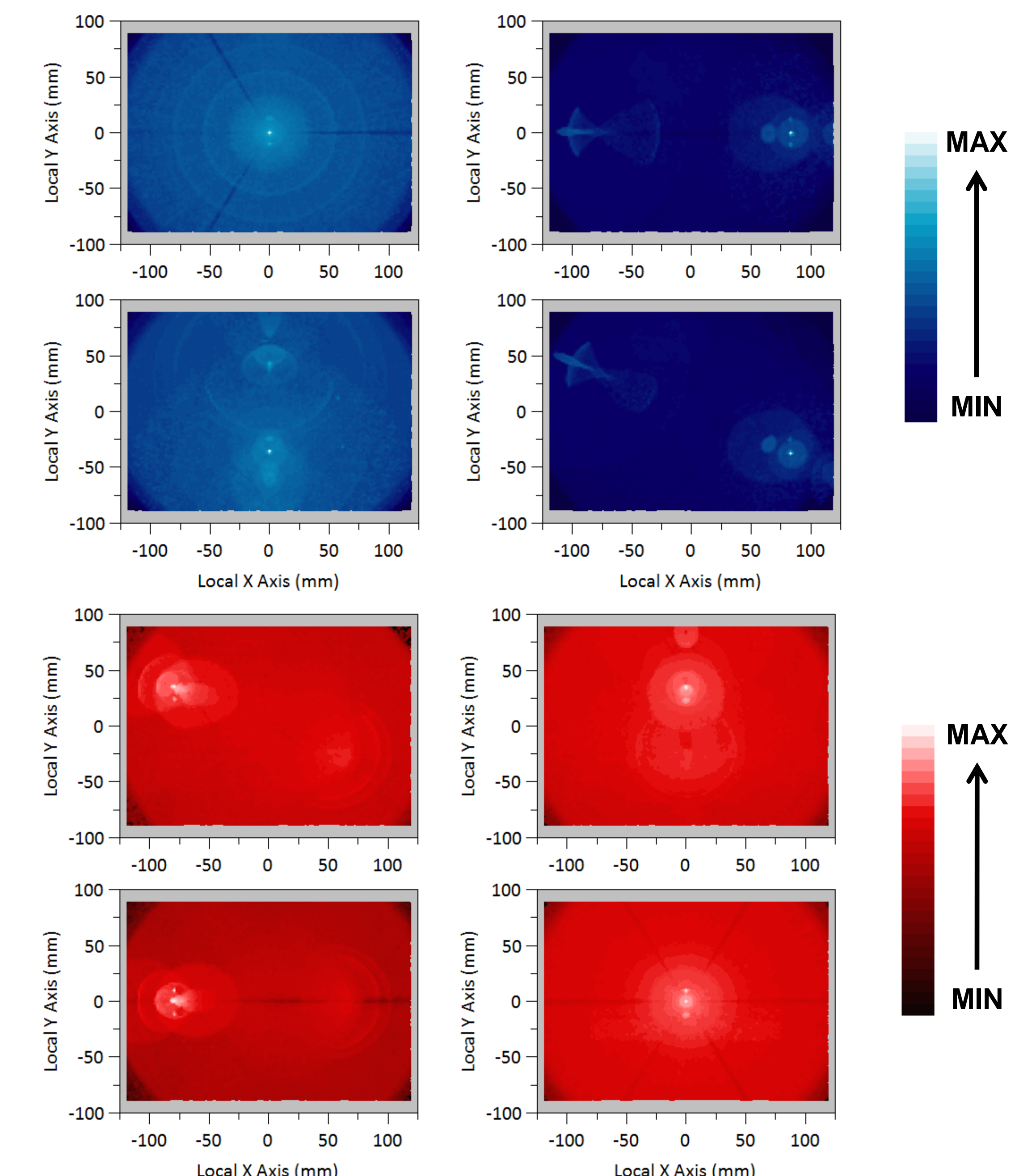


Figure 5. Ghost image irradiance (blue – top; red – bottom)

CONCLUSIONS

A preliminary stray light analysis of the imaging mode configuration of the TMT/MOBIE instrument has been completed. A complex opto-mechanical model containing key components of the dome, telescope, and instrument has been constructed. Analysis has shown the stray light background is dominated by the optical surface contributions, particularly from sources within the instrument field of view. The dome interior structures contribute to the stray light background at a comparatively low level.

Similar stray light analyses of the spectroscopic operating modes are planned for future work.

ACKNOWLEDGMENTS

The authors gratefully acknowledge the support of the TMT partner institutions. They are the Association of Canadian Universities for Research in Astronomy (ACURA), the California Institute of Technology and the University of California. This work was supported as well by the Gordon and Betty Moore Foundation, the Canada Foundation for Innovation, the Ontario Ministry of Research and Innovation, the National Research Council of Canada, the Natural Sciences and Engineering Research Council of Canada, the British Columbia Knowledge Development Fund, the Association of Universities for Research in Astronomy (AURA) and the U.S. National Science Foundation.

REFERENCES

- [1] Bernstein, R.A., Bigelow, B. C., "An optical design for a wide-field optical spectrograph for TMT," Proc. SPIE 7014, 70141G, (2008).
- [2] Harvey, J. E., "Light scattering characteristics of optical surfaces," Proc. SPIE 0107, 41-47 (1977).
- [3] Bennett, J., Mattsson, L., [Introduction to Surface Roughness and Scattering], Optical Society of America, (1999).
- [4] Spyak, P., et al, "Scatter from particulate-contaminated mirrors. Parts 1-4," Optical Engineering, Vol. 31, No. 8, (1992).
- [5] IEST, "IEST-STD-CC1246C: Product cleanliness levels and contamination control program," Institute of Environmental Sciences and Technology/IEST, (2002).